

Constraints on the recent rate of lunar ejecta breakdown and implications for crater ages

Rebecca R. Ghent^{1,2}, Paul O. Hayne³, Joshua L. Bandfield⁴, Bruce A. Campbell⁵, Carlton C. Allen⁶, Lynn M. Carter⁷, and David A. Paige⁸

¹Department of Earth Sciences, University of Toronto, 22 Russell Street, Toronto, Ontario M5S 3B1, Canada

²Planetary Science Institute, 1700 East Fort Lowell, Suite 106, Tucson, Arizona 85719, USA

³Jet Propulsion Laboratory, California Institute of Technology, Pasadena, California 91109, USA

⁴Space Science Institute, Boulder, Colorado 80301, USA

⁵Center for Earth and Planetary Studies, Smithsonian Institution, Washington, D.C. 20013, USA

⁶NASA Johnson Space Center, Houston, Texas 77058, USA

⁷NASA Goddard Space Flight Center, Greenbelt, Maryland 20771, USA

⁸Department of Earth and Space Sciences, University of California–Los Angeles, Los Angeles, California 90095, USA

ABSTRACT

We present a new empirical constraint on the rate of breakdown of large ejecta blocks on the Moon based on observations from the Lunar Reconnaissance Orbiter (LRO) Diviner thermal radiometer. We find that the rockiness of fresh crater ejecta can be quantified using the Diviner-derived rock abundance data set, and we present a strong inverse correlation between the 95th percentile value of the ejecta rock abundance (RA_{95/5}) and crater age. For nine craters with published model ages derived from crater counts on their continuous ejecta, RA_{95/5} decreases with crater age, as (age [m.y.])^{-0.46}. This result implies shorter rock survival times than predicted based on downward extrapolation of 100 m crater size-frequency distributions, and represents a new empirical constraint on the rate of comminution of large rocks not previously analyzed experimentally or through direct observation. In addition, our result provides a new method for dating young lunar craters.

INTRODUCTION

Understanding the regolith of the Moon and other planetary bodies is a central goal of planetary science because, in most cases, the regolith is what we sense with remote observations, and it thus shapes our understanding of the underlying body. A planet's regolith contains a record of bombardment at all scales, as well as materials implanted by solar wind and cosmic radiation, and therefore has much to tell us about the sources of those materials (Lucey, 2006). In addition, space weathering processes, which profoundly influence interpretations of remote observations, are intimately tied to regolith production and evolution. Fundamental questions surrounding regolith production and overturn on small Solar System bodies remain to be answered, and the rate of new regolith production from breakdown of fresh rock surfaces is an important example. The dominant process by which lunar ejecta blocks are transformed into low density, fine-grained regolith material is mechanical breakdown resulting from bombardment by small meteoroids (e.g., Hörz and Cintala, 1997). Despite the existence of radiometric dates for a small number of lunar rock and regolith samples from known locations, current understanding of the rate at which this process occurs is, for large rocks, limited by the difficulty of replicating it experimentally.

In this work, we present a new empirical estimate for the time-dependent rate of rock breakdown on the Moon based on data from the Lunar Reconnaissance Orbiter (LRO) Diviner

thermal infrared radiometer. Specifically, we investigate the age-dependent characteristics of crater ejecta as a measure of this process.

The properties of crater ejecta blankets have been studied using images and other data for 50 years, but quantifying ejecta rock abundances (and thus, analyzing the time evolution of rockiness) has involved a laborious process of manual rock counting that is dependent on image availability, quality, and illumination, all of which have limited the data available for analysis. Earth-based and orbital radar data have provided an independent means for ejecta analysis; for example, the elevated radar backscatter and circular polarization ratio signatures associated with rocky ejecta have been used to characterize impact craters and processes (Thompson et al., 1979, 1981; Ghent et al., 2005; Bell et al., 2012; Neish et al., 2013). In addition, radar provides information about the shape distribution of ejecta blanket rocks (e.g., Campbell, 2012). However, radar signatures originate from depths ranging from the surface to tens of meters in depth, and so we cannot at present distinguish between diffuse scattering arising from blocks on the surface and that from blocks buried beneath a thin layer of regolith. This is important because rocks partially or wholly buried under even a thin layer of regolith are shielded from the constant bombardment by small impactors that is experienced by exposed rocks.

Nighttime observations by LRO's Diviner instrument allow an independent estimate of the surface rock population (Bandfield et al., 2011).

Here, we investigate the Diviner-derived surface rock abundance for ejecta blankets associated with craters with model ages (derived from size-frequency distributions of superposed small craters) ranging from ca. 10 to 1000 Ma. We establish a quantitative relationship between surface rockiness and model age that represents a new empirical estimate for the time-dependent rate of large ejecta breakdown, and provides a new method for dating young lunar craters.

METHOD

Rock Abundance

Diviner-derived rock abundance estimates are calculated using the discrepancy between nighttime brightness temperatures reported by Diviner's thermal channels for fields of view that contain mixtures of warm rocks and cooler regolith. Diviner's short-wavelength thermal infrared detectors measure higher temperatures than do the longer-wavelength detectors for a given scene containing both rocks and fine-grained materials. Using this discrepancy, Bandfield et al. (2011) solved simultaneously for: the areal fraction of each scene occupied by exposed rocks ~1 m and larger (hereafter called rock abundance, or RA); and the temperature of the fines, using modelled rock temperatures as inputs. Here, we use RA values calculated using Diviner observations spanning 46 monthly mapping cycles covering the period from 5 July 2009 through 2 September 2012, and sampled at 128 pixels per degree (~240 m/px at the equator). We investigate characteristic RA values as a function of crater model ages for the ejecta blankets of nine large craters with published ages (Table 1). All craters used in this study are sufficiently large to have penetrated the entire regolith, so that variations in regolith thickness do not influence the results.

In order to understand the time evolution of characteristic ejecta RA values, we first examine RA values for the background regolith away from crater ejecta. We find that the regolith generally shows low RA values (e.g., Fig. 1; Table 2) with little variation globally (cf. Band-

TABLE 1. STUDY CRATER LOCATIONS, SIZES, AND AGES

Crater	Lat (°N)	Lon (°E)	Diameter (km)	Model age (Ma)	Reference
Aristarchus	23.7	312.5	40.0	175 –9.1/+8.8	Zanetti et al., 2011
Byrgius A	–24.6	296.2	18.7	47 ± 14.1	Morota et al., 2009
Copernicus	9.6	339.9	97.0	797 –52/+51	Hiesinger et al., 2012
Giordano Bruno	36.0	102.9	22.1	4 ± 1.2	Morota et al., 2009
Jackson	22.1	196.7	72.1	147 ± 3.8	van der Bogert et al., 2010
King	4.9	120.5	77.0	992 –89/+87	Ashley et al., 2012
Moore F	37.3	185.0	23.3	41 ± 12.3	Morota et al., 2009
Necho	–5.3	123.3	33.0	80 ± 24	Morota et al., 2009
Tycho	–43.3	348.8	86.0	85 –18/+15	Hiesinger et al., 2012

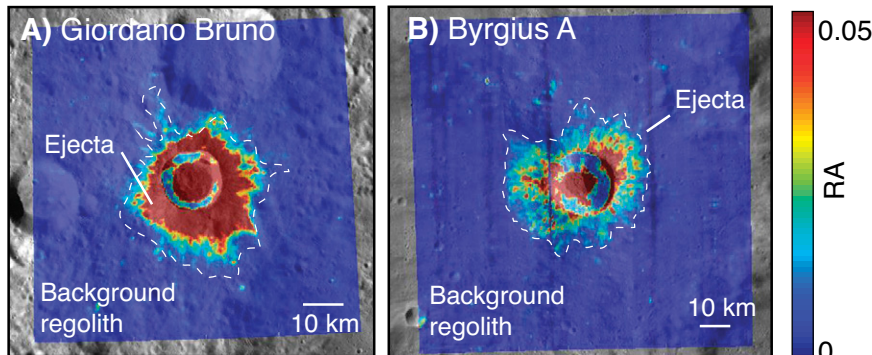


Figure 1. Lunar craters Giordano Bruno (A) and Byrgius A (B) (see Table 1). Diviner-derived rock abundance (RA; areal fraction occupied by exposed rocks) in color is overlain on Lunar Reconnaissance Orbiter Wide-Angle Camera mosaic.

TABLE 2. ROCK ABUNDANCE DISTRIBUTION CHARACTERISTICS FOR STUDY CRATERS

Crater	Ejecta rock abundance			Background rock abundance			
	Mean	Median	RA _{95/5}	Mean	Median	s	RA _{95/5}
Giordano Bruno	0.033	0.011	0.1244	0.0049	0.0049	0.0025	0.0067
Moore F	0.020	0.012	0.0580	0.0041	0.0041	0.0011	0.0059
Byrgius A	0.018	0.013	0.0468	0.0043	0.0042	0.0017	0.0065
Necho	0.014	0.010	0.0369	0.0045	0.0044	0.0012	0.0063
Tycho	0.014	0.010	0.0370	0.0037	0.0035	0.0027	0.0060
Jackson	0.011	0.010	0.0202	0.0041	0.0040	0.0014	0.0058
Aristarchus	0.014	0.011	0.0309	0.0056	0.0045	0.0056	0.0109
Copernicus	0.006	0.006	0.0117	0.0039	0.0034	0.0050	0.0061
King	0.006	0.006	0.0103	0.0044	0.0042	0.0025	0.0063

Rock abundance is areal fraction of each Diviner pixel covered by exposed rocks. RA_{95/5} is 95th percentile value of ejecta rock abundance.

field et al., 2011); mean values for the highland terrains used in this study are 0.004–0.005 (i.e., 0.4–0.5% of each pixel area covered by exposed rocks), and 0.004–0.006 for mare terrains (Fig. 2; Table 2). These characteristics indicate that most of the Moon’s surface has a negligible population of meter-scale rocks.

By contrast, rocky ejecta blankets show a significant number of Diviner pixels with high RA values, leading to RA distributions that are strongly skewed to the right, with long tails reflecting characteristically higher values (Fig. 3; Table 2). Unlike the background regolith values, ejecta RA values are not normally

or lognormally distributed. Therefore, statistical parameters used to represent the central tendency of a population or sample (mean, median) do not adequately represent the characteristics of the ejecta RA distribution. In order to quantify the rockiness of crater ejecta as a function of age, we need to capture the variation that occurs in the right-hand tail of the RA distribution. Therefore, for each ejecta blanket we use the 95th percentile value as a measure of the population maximum. This value, denoted RA_{95/5}, is the threshold value separating the highest 5% of a given crater’s ejecta RA values from the lower 95%. This measure has been used in analysis

of populations with similar properties in other fields, such as organismal body size variations with temperature (Chapelle and Peck, 1999), or novelty detection for mechanical damage analysis (Sohn et al., 2005). RA_{95/5} values for the study craters and the surrounding regolith are shown in Table 2.

For each crater and its surrounding terrain, we calculated mean and median RA values (and standard deviation for the background terrain) and RA_{95/5}, excluding all terrain inside the crater’s topographic rim, where mass wasting from steep slopes is likely to refresh the surface rock population (e.g., Fig. 1). We omitted large melt ponds, as discussed below.

Crater Ages

The craters used in this study (Table 1) have published model ages derived from counts of small craters superposed on their ejecta, performed using new, high-resolution images from the SELENE Terrain Camera onboard the Japanese Kaguya orbiter, and the LRO Wide-Angle Camera (WAC) and Narrow-Angle Camera (NAC). For some craters (notably, King crater), counts of small craters on melt ponds yield ages that are widely discrepant from those obtained from counts on ejecta blankets, due at least in part to variations in mechanical strength of the target (regolith versus impact melt; van der Bogert et al., 2010). To avoid possible complications associated with including these terrains in our analysis, we removed large melt deposits from our data set.

The errors on the ages reported in Table 1 are associated with inherent uncertainties in crater count chronologies (e.g., Hiesinger et al., 2012). The regression we present in the next section was calculated independently of these errors; however, to account for their potential influence, we calculated the 95% confidence belt on the regression (Fig. 4), which represents the range in which 95% of regressions calculated using repeated samples of nine hypothetical craters spanning this age range would fall. We discuss this further in the next section.

RESULTS AND DISCUSSION

Figure 4 shows the log-log regression of RA_{95/5} versus age for our study craters; the regression yields the relationship

$$RA_{95/5} = 0.27 \times (\text{age [m.y.]})^{-0.46}, \quad (1)$$

with an R² value of 0.96. This indicates a strong inverse power-law correlation between crater ejecta rockiness and age for craters younger than ca. 1 Ga. Removal of the isolated point representing Giordano Bruno yields a slope of –0.51 (R² = 0.95), indicating that this point does not exert undue influence on the regression. With increasing age, crater ejecta RA distributions narrow, becoming less strongly right

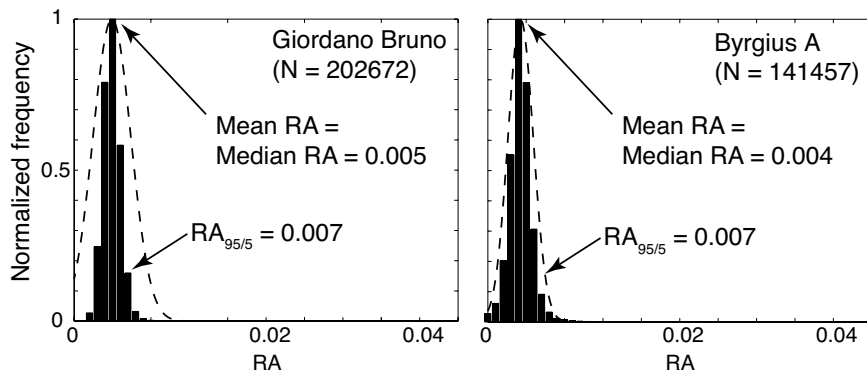


Figure 2. Histograms of rock abundance (RA) values for background regolith at lunar craters Giordano Bruno and Byrgius A; mean RA, median RA, and $RA_{95/5}$ (95th percentile value of ejecta rock abundance) values are indicated. Here, mean and median are equal. Dashed curves represent normal distributions centered at the mean values. N is number of pixels represented.

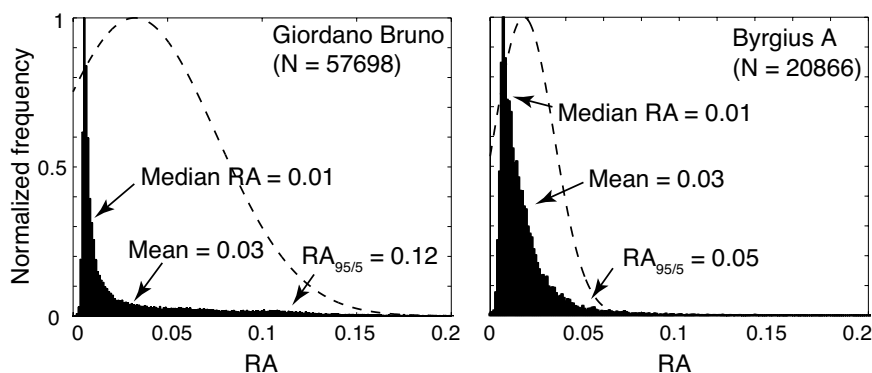


Figure 3. Histograms of rock abundance (RA) values for lunar craters Giordano Bruno and Byrgius A ejecta; mean RA, median RA, and $RA_{95/5}$ (95th percentile value of ejecta rock abundance) values are indicated. Dashed curves represent normal distributions centered at the mean values. N is number of pixels represented.

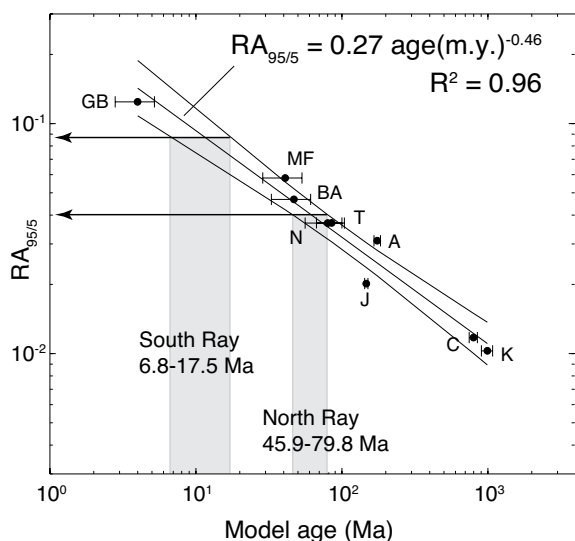


Figure 4. Log-log regression of 95th percentile value of ejecta rock abundance ($RA_{95/5}$) versus crater age for craters with published model ages used in this study; data (including errors on crater ages) are given in Tables 1 and 2. 95% confidence intervals on the regression are shown. Calculated RA values and corresponding ages for craters North Ray and South Ray at Apollo 16 landing site are also shown. Because these two ejecta blankets are so small (N = 231 and 191 pixels, respectively), ages for these two craters were calculated using maximum RA values rather than $RA_{95/5}$. Crater abbreviations: A—Aristarchus; BA—Byrgius A; C—Copernicus; GB—Giordano Bruno; J—Jackson; K—King; MF—Moore F; N—Necho; T—Tycho.

skewed and closer to normal, until they become indistinguishable from the background regolith (compare Figs. 2 and 3).

Equation 1 implies much shorter survival times for rocks >1 m in diameter than predicted

by extrapolating estimates derived for smaller rocks from earlier studies (e.g., Shoemaker et al., 1970; Gault et al., 1972; Hörz et al., 1974, 1975). Those previous estimates were derived from extrapolation of the observed 100 m–1 km

crater size-frequency distribution down to millimeter sizes (e.g., Shoemaker et al., 1970), to calculate the probability of destruction of a rock by sandblasting by much smaller impactors and by catastrophic rupture by impactors comparable to the size of the target rock. Consistent with our result, experiments have shown that large rocks are effectively weaker in collisions with projectiles than small rocks (e.g., Housen and Holsapple, 1999; Housen and Voss, 2000), but the underlying cause of this phenomenon is not completely understood, and few experiments on rocks as large as those reflected in the Diviner RA data set have been performed. In addition to variations in effective rock strength, other processes, such as weakening by thermal stresses arising from diurnal heating and cooling (Delbo et al., 2014), should contribute as well. Meter-sized rock survival times presented by Basilevsky et al. (2013) for Apollo and Lunakhod landing site craters with diameter <1 km and up to 300 m.y. in age, estimated via morphological analysis from Lunar Reconnaissance Orbiter Camera (LROC) NAC images and using cosmic ray exposure ages, are also shorter than those predicted by, e.g., Hörz et al. (1975). Basilevsky et al.'s (2013) results are thus qualitatively consistent with the quantitative model presented in this paper.

An important implication of our result is that it provides a completely new and independent method for dating young lunar craters. Comparison of cosmic ray exposure ages for North and South Ray craters at the Apollo 16 landing site (50 Ma and 2 Ma, respectively; Arvidson et al., 1975) with ages predicted by our method (46–80 Ma for North Ray and 7–18 Ma for South Ray; Fig. 4) support this idea. Although North and South Ray craters are much smaller than the large craters used in our study, and therefore probably started with fewer and smaller ejecta blocks, our calculated ages are broadly consistent with the cosmic ray exposure ages. This demonstrates the potential for applying our method, given a crater size-appropriate calibration curve, to determine ages for even small lunar craters. Future work will build on this result to evaluate its implications for the lunar impact rate.

ACKNOWLEDGMENTS

This work was supported by a Discovery grant from the National Science and Engineering Research Council of Canada to Ghent, and by the NASA Lunar Reconnaissance Orbiter Participating Scientist program. We thank David Blewett and an anonymous reviewer for helpful comments.

REFERENCES CITED

- Arvidson, R., Crozaz, G., Drozd, R.J., Hohenberg, C.M., and Morgan, C.J., 1975, Cosmic ray exposure ages of features and events at the Apollo landing sites: *The Moon*, v. 13, p. 259–276, doi:10.1007/BF00567518.
- Ashley, J.W., et al., 2012, *Geology of the King crater region: New insights into impact melt dynamics*

- on the Moon: *Journal of Geophysical Research*, v. 117, E00H29, doi:10.1029/2011JE003990.
- Bandfield, J.L., Ghent, R.R., Vasavada, A.R., Paige, D.A., Lawrence, S.J., and Robinson, M.S., 2011, Lunar surface rock abundance and regolith fines temperatures derived from LRO Diviner Radiometer data: *Journal of Geophysical Research*, v. 116, E00H02, doi:10.1029/2011JE003866.
- Basilevsky, A.T., Head, J.W., and Hörz, F., 2013, Survival times of meter-sized boulders on the surface of the Moon: *Planetary and Space Science*, v. 89, p. 118–126, doi:10.1016/j.pss.2013.07.011.
- Bell, S.W., Thomson, B.J., Dyar, M.D., Neish, C.D., Cahill, J.T.S., and Bussey, D.B.J., 2012, Dating small fresh lunar craters with Mini-RF radar observations of ejecta blankets: *Journal of Geophysical Research*, v. 117, E00H30, doi:10.1029/2011JE004007.
- Campbell, B.A., 2012, High circular polarization ratios in radar scattering from geologic targets: *Journal of Geophysical Research*, v. 117, E06008, doi:10.1029/2012JE004061.
- Chapelle, G., and Peck, L.S., 1999, Polar gigantism dictated by oxygen availability: *Nature*, v. 399, p. 114–115, doi:10.1038/20099.
- Delbo, M., Libourel, G., Wilkerson, J., Murdoch, N., Michel, P., Ramesh, K.T., Ganino, C., Verati, C., and Marchi, S., 2014, Thermal fatigue as the origin of regolith on small asteroids: *Nature*, v. 508, p. 233–236, doi:10.1038/nature13153.
- Gault, D.E., Hörz, F., and Hartung, J.B., 1972, Effects of microcratering on the lunar surface: *Proceedings of the 3rd Lunar Science Conference*, Houston, Texas, 10–13 January 1972, Volume 3, (A73-19676 07-30): Cambridge, Massachusetts, MIT Press, p. 2713–2734.
- Ghent, R.R., Leverington, D.W., Campbell, B.A., Hawke, B.R., and Campbell, D.B., 2005, Earth-based observations of radar-dark crater haloes on the Moon: Implications for regolith properties: *Journal of Geophysical Research*, v. 110, E02005, doi:10.1029/2004JE002366.
- Hiesinger, H., van der Bogert, C.H., Pasckert, J.H., Funcke, L., Giacomini, L., Ostrach, L.R., and Robinson, M.S., 2012, How old are young lunar craters?: *Journal of Geophysical Research*, v. 117, E00H10, doi:10.1029/2011JE003935.
- Hörz, F., and Cintala, M., 1997, The Barringer Award Address presented 1996 July 25, Berlin, Germany: Impact experiments related to the evolution of planetary regoliths: *Meteoritics & Planetary Science*, v. 32, p. 179–209, doi:10.1111/j.1945-5100.1997.tb01259.x.
- Hörz, F., Schneider, E., and Hill, R.E., 1974, Micro-meteoroid abrasion of lunar rocks: A Monte-Carlo simulation: *Proceedings of the 5th Lunar Science Conference*, Houston, Texas, 18–22 March 1974, Volume 3, (A75-39540 19-91): New York, Pergamon Press, Inc., p. 2397–2412.
- Hörz, F., Schneider, E., Gault, D.E., Hartung, J.B., and Brownlee, D.E., 1975, Catastrophic rupture of lunar rocks: A Monte Carlo simulation: *Earth, Moon, and Planets*, v. 13, p. 235–258, doi:10.1007/BF00567517.
- Housen, K.R., and Holsapple, K.A., 1999, Scale effects in strength-dominated collisions of rocky asteroids: *Icarus*, v. 142, p. 21–33, doi:10.1006/icar.1999.6206.
- Housen, K.R., and Voss, M.E., 2000, Scale-dependent outcomes in collisional fragmentation of basalt: Lunar and Planetary Institute Science Conference, Houston, Texas, 13–17 March 2000, Abstract 1495.
- Lucey, P., 2006, Understanding the lunar surface and space-moon interactions: *Reviews in Mineralogy and Geochemistry*, v. 60, p. 83–219, doi:10.2138/rmg.2006.60.2.
- Morota, T., et al., 2009, Formation age of the lunar crater Giordano Bruno: *Meteoritics & Planetary Science*, v. 44, p. 1115–1120, doi:10.1111/j.1945-5100.2009.tb01211.x.
- Neish, C.D., Blewett, D.T., Harmon, J.K., Coman, E.I., Cahill, J.T.S., and Ernst, C.M., 2013, A comparison of rayed craters on the Moon and Mercury: *Journal of Geophysical Research*, v. 118, p. 2247–2261, doi:10.1002/jgre.20166.
- Shoemaker, E.M., Hait, M.H., Swann, G.A., Schleicher, D.L., Schaber, G.G., Sutton, R.L., Dahlem, D.H., Goddard, E.N., and Waters, A.C., 1970, Origin of the lunar regolith at Tranquillity Base: *Geochimica et Cosmochimica Acta*, v. 1, Supplement, p. 2399.
- Sohn, H., Allen, D.W., Worden, K., and Farrar, C.R., 2005, Structural damage classification using extreme value statistics: *Journal of Dynamic Systems, Measurement, and Control*, v. 127, p. 125–132, doi:10.1115/1.1849240.
- Thompson, T.W., Roberts, W.J., Hartmann, W.K., Shorthill, R.W., and Zisk, S.H., 1979, Blocky craters: Implications about the lunar megaregolith: *The Moon and the Planets*, v. 21, p. 319–342, doi:10.1007/BF00897360.
- Thompson, T.W., Zisk, S.H., Shorthill, R.W., Schultz, P.H., and Cutts, J.A., 1981, Lunar craters with radar bright ejecta: *Icarus*, v. 46, p. 201–225, doi:10.1016/0019-1035(81)90209-8.
- van der Bogert, C.H., Hiesinger, H., McEwen, A.S., Dundas, C., Bray, V., Robinson, M.S., Plescia, J.B., Reiss, D., Klemm, K., and the LROC Team, 2010, Discrepancies between crater size-frequency distributions on ejecta and impact melt pools at lunar craters: An effect of differing target properties?: 41st Lunar and Planetary Science Conference, The Woodlands, Texas, 1–5 March 2010: <http://www.lpi.usra.edu/meetings/lpsc2010/pdf/2165.pdf>.
- Zanetti, M., Hiesinger, H., van der Bogert, C.H., Reiss, D., and Jolliff, B.L., 2011, Aristarchus crater: Mapping of impact melt and absolute age determination: 42nd Lunar and Planetary Science Conference, The Woodlands, Texas, 7–11 March 2011: <http://www.lpi.usra.edu/meetings/lpsc2011/pdf/2330.pdf>.

Manuscript received 28 May 2014

Revised manuscript received 6 September 2014

Manuscript accepted 11 September 2014

Printed in USA